Stochastic Environmental Research and Risk Assessment (2026) 40:21
https://doi.org/10.1007/s00477-025-03137-3

ORIGINAL PAPER

An integrated regionalization framework for incorporating flood seasonality into agricultural flood risk assessments

Anna Rita Scorzini[1] · **Charlie Dayane Paz Idarraga**[2] · **Daniela Molinari**[2]

Received: 5 August 2025 / Accepted: 20 November 2025 / Published online: 8 January 2026

Abstract
Flood risk to agriculture is strongly influenced by the timing of inundation relative to crop development stages, making flood seasonality a critical but often overlooked component in damage estimation. This study introduces a generalizable regionalization framework that combines hydrological clustering and machine learning to incorporate seasonal flood probability into agricultural risk assessment. The approach involves identifying clusters of gauged catchments with similar patterns of intra-annual flood occurrence and using supervised classification to extrapolate these seasonal regimes to ungauged catchments based on their physical attributes. The resulting spatially distributed maps of monthly flood probability can be then integrated with a flood damage model to calculate expected annual losses and support risk estimates across entire river districts. The proposed framework, applied in this study to the Po River District (Italy) for illustrative purposes, is scalable and adaptable to different regions, contributing to more robust and context-sensitive adaptation planning in agriculture. Results highlight the importance of accounting for flood seasonality in cost-benefit analyses within agricultural contexts, as neglecting intra-annual variability can lead to overestimated damage projections and suboptimal mitigation strategies.

Keywords Catchment · Regionalization · Flood seasonality · Damage · Crop

1 Introduction

Flood events are a major driver of economic losses in agricultural systems, especially in regions with intensive cultivation, where damage to crops and soil can severely impact production and farm income (FAO 2023; Kim et al. 2023). Accurate flood risk assessments are then essential for supporting effective disaster risk reduction, climate adaptation strategies and resilience policies (Yildirim and Demir 2022). In such assessments, flood damage models play a central role by linking hazard variables and vulnerability factors to estimate expected economic losses (Merz et al. 2010). While more standard models have been developed for other economic sectors (e.g., residential sector), their application to agriculture, and in particular to crop damage, presents distinctive challenges. Differently from buildings, which exhibit a more static vulnerability, crop sensitivity to flooding is indeed tightly linked to the development stage of the plants at the time of inundation (Förster et al. 2008; Bremond et al. 2013, 2022; Vozinaki et al. 2015; Molinari et al. 2019; Scorzini et al. 2021). This results in widely varying damage outcomes depending on the timing of the flood within the growing season: the same event can cause negligible, moderate, or severe losses depending on whether it occurs during sowing, flowering or harvesting. As such, conventional flood hazard representations based on annual exceedance probability (i.e., return periods) are poorly suited for agricultural damage assessments, as they fail to account for the seasonal dynamics of flood exposure relative to crop development. This calls for a shift toward seasonally-explicit, monthly-based risk estimations (Molinari et al. 2019; Scorzini et al. 2021; Lazzarin et al. 2022), where expected annual losses are estimated as the probability-weighted sum of monthly losses, with weights reflecting the likelihood of flooding in each month.

✉ Anna Rita Scorzini
annarita.scorzini@univaq.it

[1] Department of Civil, Environmental and Architectural Engineering, University of L'Aquila, 67100 L'Aquila, Italy

[2] Department of Civil and Environmental Engineering, Politecnico di Milano, 20133 Milan, Italy

However, achieving this level of temporal detail in flood hazard assessments can be particularly challenging in data-scarce regions, where hydrological records are sparse or unavailable. Moreover, hydrological systems are inherently heterogeneous, exhibiting substantial variability in both their physical properties and their response behaviors (Sivakumar and Singh 2012; Blöschl et al. 2013). In this context, regionalization techniques offer a solution for inferring flood regime characteristics in ungauged catchments, based on similarity criteria relying on the assumption that the aggregated hydrologic response reflects dominant physiographic and climatic attributes of the areas (e.g., Merz and Blöschl 2004; Rao and Srinivas 2006, 2008; Coopersmith et al. 2012; Blöschl et al. 2013; Razavi and Coulibaly 2013; Salinas et al. 2013; Gao et al. 2018; Drissia et al. 2022).

To support hydrologic regionalization, various catchment classification frameworks have been proposed in the literature, typically based either on physiographic and climatic descriptors or on hydrologic response signatures. Approaches grounded in physical attributes (such as topography, geology, land use) have the advantage of wide spatial coverage and data accessibility, making them particularly suitable for large-scale applications. For instance, Winter (2001) introduced the concept of hydrologic landscapes, identifying groups of catchments with similar climate, topography and geology, under the assumption that such similarity would translate into similar hydrologic behavior. This concept was later operationalized by Wolock et al. (2004), who delineated 20 hydrologically distinct regions across the USA using over 40,000 spatial units of approximately 200 km². Other contributions have emphasized the structural and functional components of catchment hydrology. For example, Buttle (2006) highlighted the importance of three hierarchical factors in determining streamflow response: hydrologic typology (partitioning of flow paths), topology (drainage connectivity) and topography (hydraulic gradients). Similarly, several studies have used soil-related or geomorphological variables to group catchments, such as in Bormann et al. (1999, 2010) or Rao and Srinivas (2006). Despite their conceptual and operational appeal, these physically based approaches do not always guarantee that similarly classified catchments will exhibit analogous hydrologic responses, as found by Merz and Blöschl (2009) when analyzing over 400 Austrian catchments. On the other hand, classification frameworks based on hydrologic response (such as flow regime characteristics or variability indices) provide a more direct link to the behavior of interest, but are inherently limited to gauged catchments. Consequently, while both approaches offer complementary strengths, neither is sufficient on its own to ensure successful information transfer or generalization. For this reason, recent efforts have increasingly focused on establishing quantitative relationships between catchment attributes and hydrologic signatures, with the aim of enabling behavioral inference in ungauged locations (Wagener et al. 2007; Sawicz et al. 2011; Kuentz et al. 2017; Fathi and Awadallah 2025).

In line with this perspective, the present study introduces a generalizable framework for incorporating flood seasonality into agricultural risk assessment through regionalization. The approach integrates unsupervised clustering and supervised machine learning to infer seasonal flood regime characteristics across large river districts. Specifically, clustering is applied to monitored sites to identify groups of catchments that exhibit similar monthly flood probability patterns. These hydrological clusters are then used to train classification models that infer the relationships between physical catchment attributes and flood seasonality. Once trained, the models can be applied to predict the flood regime in ungauged catchments based solely on their physical descriptors, allowing a spatial transfer of seasonally-resolved flood hazard data for crop damage modeling.

In this study, the proposed framework is implemented for the Po River District (Italy) to demonstrate its broader applicability and usefulness for improving agricultural flood risk assessment and related decision-making. The regionalization of flood seasonality is applied to the entire district and coupled with a crop damage model for a system of two APSFRs (Area of Potential Significant Flood Risk), in order to illustrate how the integration of seasonal flood hazard information can influence expected losses and the outcomes of cost-benefit analyses for mitigation planning. Beyond this application, the main novelty of the framework lies in the integration of its components into a coherent and transferable workflow, enabling (i) the regionalization of monthly resolved flood probabilities to ungauged basins and (ii) their incorporation into crop-specific damage modeling. By linking these traditionally separate domains, the framework consistently propagates seasonal hazard information into impact and economic evaluations, resulting in more physically consistent and policy-relevant risk estimates.

2 Methodology

2.1 Overview of the proposed framework

The methodological framework developed in this study integrates hydrological regionalization with crop damage modeling to support agricultural flood risk assessments in data-scarce contexts. It is structured into two sequential components, where the first provides one of the key input required by the second (Fig. 1).

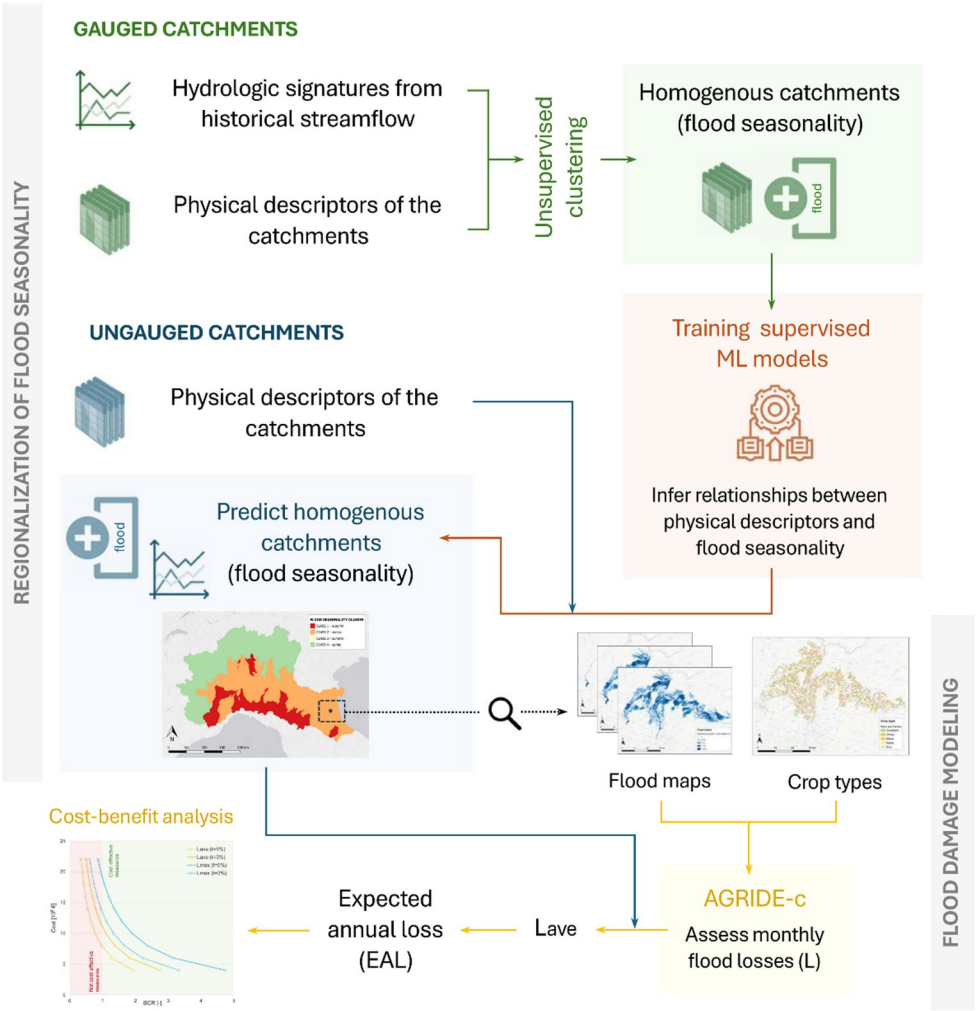

Fig. 1 Overview of the proposed framework.

The first component focuses on the regionalization of seasonally-resolved flood regime characteristics, with the objective of generating spatially distributed monthly flood probabilities across a (large-scale) river district.

The process begins with the extraction of hydrologic signatures from observed streamflow records at gauged locations, along with physical descriptors of the corresponding upstream catchment. These features are then used to group the catchments into homogeneous classes through unsupervised clustering.

To generalize the relationship between physical features and flood seasonality, supervised machine learning models are trained using data from gauged basins, where both types of information are available. Once trained, these models are applied to predict the flood regime characteristics in ungauged areas by leveraging only their physical attributes. The resulting output consists of a classification of the study area into homogeneous regions based on flood seasonality, each associated with a representative profile of monthly flood probabilities, offering a seasonally explicit hazard representation for agricultural risk analysis.

The second component of the framework uses the seasonally-resolved flood hazard information to assess agricultural flood risk. Specifically, expected annual loss (EAL) is computed as the probability-weighted sum of monthly losses, where the weights correspond to the monthly flood probabilities obtained through regionalization. Monthly losses for the different exposed crops are estimated using a flood damage model (i.e., AGRIDE-c, Molinari et al. (2019), which accounts for key hydraulic variables (such as inundation depth and duration, flow velocity, etc.) associated with different return period flood scenarios as well as time-varying vulnerability linked to the phenological phases of the crops.

2.2 Study area and data availability

The application of the proposed framework is illustrated for the Po River District, located in Northern Italy (Fig. 2). Covering an area of over 70,000 km², the district features a wide range of physiographic and climatic conditions, extending from the Alpine range to the Adriatic coastal plain. It includes several flood-prone areas and a high density of

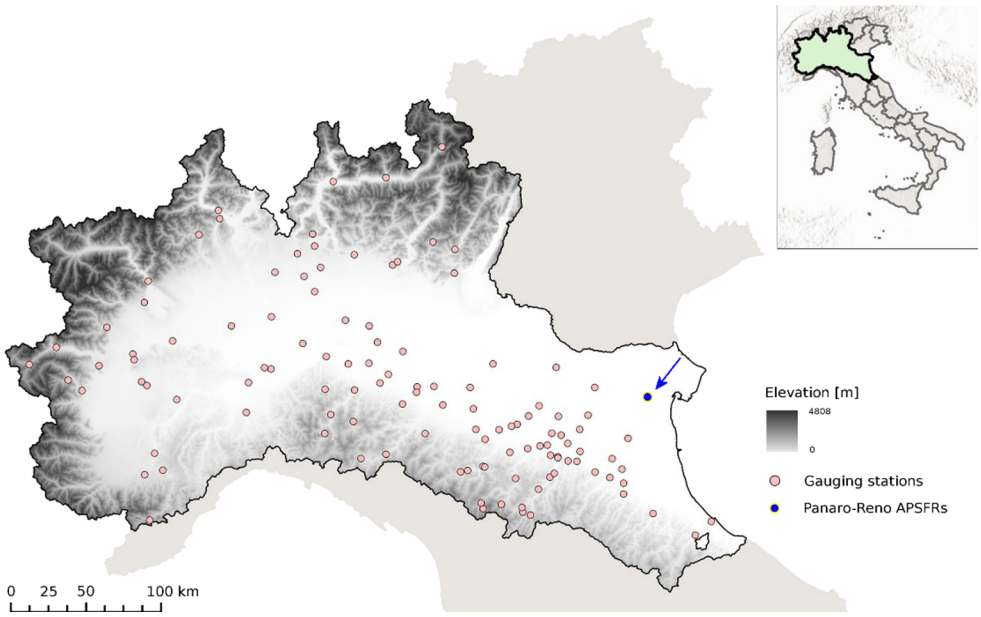

Fig. 2 The Po River District, with indication of the considered hydrometric stations and the localization of the case-study area for the small-scale flood damage application.

agricultural land, making it a critical region in terms of flood risk to crops. Within the district, 31 APSFRs (Area of Potential Significant Flood Risk) have been delineated under the European Floods Directive framework, reflecting historical exposure to significant flood events and socio-economic vulnerability.

Hydrologically, the district is characterized by strong spatial heterogeneity in flood-generating mechanisms. In the northern mountainous and hilly zones, floods are primarily driven by rapid snowmelt and orographic rainfall, while in the central and southern lowlands, prolonged rainfall events and fluvial backwater conditions play a dominant role (De Michele and Rosso 2002; Montanari 2012). This complexity makes the Po River District an ideal testbed for developing and assessing regionalization techniques and risk assessment frameworks.

The regionalization component of the methodology is based on monthly flow data - either discharge or hydrometric level - collected from a network of monitoring stations distributed throughout the district. An initial screening identified 120 hydrometric stations (Fig. 2) with sufficiently long and complete time series (with a minimum length of 20 years). For each station, the month corresponding to the annual peak flow is extracted for each year in the observation period. These data are then used to compute the empirical probability of annual peak flow occurrence in each calendar month, providing a monthly flood occurrence profile for each site. Each gauging station is further characterized by a set of physical attributes (described in Sect. 2.3.1 and listed in Table 1) representing the physical and land cover features of the contributing catchment area. These are derived from Italy's 10-meter resolution Digital Elevation Model (Tarquini et al. 2023) and land use data from the CORINE Land Cover dataset, provided by the Copernicus Land Monitoring Service. Summary statistics of the full set of physical descriptors (minimum, maximum and mean values) are reported in Table 1. In addition, the presence of upstream flow regulation is considered by including information on major hydraulic structures, extracted from the national dam register maintained by the Italian General Directorate for Dams and Water Infrastructures. Specifically, a binary variable is used to indicate the presence or absence of dams intersecting the main channel within each catchment. Notably, more than 30% of the analyzed basins include at least one of such structure, underlining the potential relevance of flow regulation effects in shaping downstream flood regimes.

As part of the agricultural risk modeling component, an illustrative case study is carried out in the Panaro-Reno APSFRs located in the southern part of the District (Fig. 2, highlighted with an arrow). In this context, spatially detailed crop data are obtained from the agricultural cadaster of the Emilia-Romagna region, which provides parcel-level information on crop type and geographic distribution. The characteristics of the flooding scenarios are derived from high-resolution inundation maps produced by the Po River District Authority for three synthetic flood scenarios with return periods of 25, 100, and 500 years. These maps include raster datasets representing flood depth at spatial resolutions of 10 m for the Reno River and 5 m for the Panaro River.

Table 1 Description of the physical features used to characterize catchments to support both the clustering of seasonal flood regimes and the supervised classification of ungauged basins.

Feature	Feature name	Description	Range of values[1]
Drainage area	Area	Total surface area of the catchment	14.9–59,970 (3631) km^2
Mean slope	Slope	Average slope across the entire catchment	0.54–35.0 (17.8) deg
Stream network density	DrainageDensity	Total stream length per unit area of the catchment	0.03–0.56 (0.31) km/km^2
Mean altitude	MeanAltitude	Hypsometric mean elevation of the catchment	43.2–2352 (801.9) m
Basin relief	Relief	Elevation difference between the highest and lowest points within the catchment	70.5–4800 (1937) m
Topographic Wetness Index (Sørensen et al. 2006)	TWI	Index indicating potential for water accumulation based on slope and upstream contributing area	7.1–14.3 (8.7)
% Forested area	ForestCover	Percentage of the catchment covered by forest vegetation (CLC3)	0–100 (57.7) %
% Impervious area	ImperviousCover	Percentage of the catchment covered by impervious surfaces (e.g., roads, buildings)	0–89 (6.6) %
Dams	Presence of upstream reservoirs	Binary indicator of whether regulation reservoirs are present upstream	0: no 1: yes

[1]The mean value is reported in parentheses

2.3 Regionalization of flood seasonality

2.3.1 Clustering of seasonal flood regimes

To identify catchments with similar intra-annual flood occurrence patterns, an unsupervised hierarchical clustering approach is adopted. The clustering is based on a set of synthetic descriptors that characterize both the timing of peak flood occurrence (i.e., month encoded as an integer between 1 for January and 12 for December) and the physical context of each catchment. The physical descriptors - listed and described in Table 1 - fall into three macro-categories: (i) drainage network organization and basin morphometry, which control hydrological response times and storage capacity; (ii) land cover characteristics, which influence infiltration rates, surface roughness and soil moisture dynamics; and (iii) presence of flow-regulating infrastructure, which directly alters natural runoff timing and peak attenuation through dams and retention structures.

Variables are selected based on their documented relevance to flood generation and seasonality, availability at the district scale and computational efforts for their assessment (e.g., Buttle 2006; Merz and Blöschl 2004; Sawicz et al. 2011; Kuentz et al. 2017).

Pairwise dissimilarities between catchments are quantified using the euclidean distance metric, while cluster formation is performed using the Ward linkage method, which minimizes within-cluster variance and tends to produce compact, balanced groups. This combination is particularly suitable for hydrological signatures that exhibit gradual seasonal gradients.

The number of clusters has been varied systematically and selected based on dendrogram inspection with attention to cluster stability and hydrological interpretability. Each cluster is interpreted as representing a typical seasonal flood regime, defined by the timing and distribution of flood probabilities throughout the year. For each cluster, a representative monthly flood probability distribution is then computed as the average of the station-specific probabilities for all gauged catchments belonging to the same cluster, providing a characteristic signature to be transferred to ungauged areas.

2.3.2 Regionalization to ungauged catchments via supervised learning

To enable the transfer of hydrological patterns to ungauged catchments across the district, a supervised classification framework is developed. The approach involves training machine learning models to identify the relationship between the characteristics of gauged sub-catchments (predictors) and their associated flood seasonality class (target), as obtained from the previous step. To allow for model transfer in ungauged areas, all sub-catchments within the Po River District (as defined according to the official delineation provided by the River District Authority) are then characterized in terms of the physical predictors listed in Table 1.

Three widely used classifiers are tested for their ability to capture the relationship between physical catchment attributes and seasonal flood regimes:

- Support Vector Machine (SVM): a kernel-based classifier that finds the optimal hyperplane separating classes in high-dimensional space (Cortes and Vapnik 1995). SVMs can handle complex decision boundaries, especially when using non-linear kernels.

- Random Forest (RF): an ensemble-based algorithm that constructs several decision trees and outputs the most frequent class prediction (Breiman 2001).
- K-Nearest Neighbors (KNN): a non-parametric model that assigns a class based on the majority vote of the k closest training samples in the feature space (Cover and Hart 1967).

An ensemble-consensus strategy is adopted to reduce model dependency and mitigate the risk of overfitting under potential data constraints, as in the study area. The approach, which consists in independently training the three classifiers and then assigning a final cluster label only when at least two models agree, is not merely a pragmatic choice for this study, but a reproducible solution for other data-scarce regionalization contexts: convergence among multiple classifiers can indeed increase confidence in the transferred seasonal label and help identifying locations where predictions are more uncertain.

Hyperparameter tuning is performed for each model using a random search procedure, including the number of estimators and maximum depth for RF, the number of neighbors for KNN and the regularization parameter and kernel type for SVM. Model performance is evaluated using a repeated holdout validation scheme: the dataset of gauged catchments is randomly split into training (70%) and test (30%) sets across 100 iterations to ensure a robust assessment and reduce sampling bias. For each model, the overall performance is evaluated using classification accuracy, macro-averaged precision and analysis of the confusion matrices. The accuracy metric measures the proportion of correctly classified instances out of the total number of predictions, while precision reflects the model's ability to avoid false positives across all classes by averaging precision values equally across them; confusion matrices provide a comprehensive understanding of classification effectiveness and help in identifying potential misclassification patterns.

The model that achieves the best overall classification performance is selected for predicting the seasonal cluster for ungauged sub-catchments, resulting in a spatially distributed map of flood regime types across the entire district. Accordingly, each ungauged catchment is assigned a representative monthly flood probability distribution, computed from the average of the distributions observed in the gauged catchments belonging to the same cluster.

In addition to predictive performance, a variable importance analysis is carried out for the different models using the mean decrease in classification accuracy (mdca) as a metric. This approach involves randomly permuting the values of each predictor variable (30 permutations per variable) and measuring the resulting decrease in classification accuracy. Variables leading to the largest drop in performance are considered the most influential in determining the seasonal flood pattern of a catchment.

2.4 Crop damage modeling

To quantify flood-induced impacts on crops, this study adopts the AGRIDE-c model (Molinari et al. 2019), a conceptual and analytical framework structured into two main components: a physical damage module, which evaluates the direct effects of flooding on crops and soils, and an economic module, which translates these impacts into monetary losses. A distinguishing feature of AGRIDE-c is its dynamic representation of crop vulnerability, which varies according to the phenological stage of the crop at the time of flooding and crop-specific tolerance thresholds. As a result, the model enables damage estimation for flood events occurring in any month of the year, thereby supporting a probabilistic risk assessment that explicitly accounts for seasonal variations in crop vulnerability and flood hazard likelihood. Originally developed for the Po River District (Molinari et al. 2019), the model has been also adapted and applied in other regional contexts (Scorzini et al. 2021; Lucaora et al. 2025).

The physical damage module estimates the reduction in agricultural output based on key flood hazard characteristics (such as inundation depth and duration, flow velocity, etc.) that affect yield quantity and quality. Physical damage is expressed as a loss in expected yield and/or market value, which directly translates into a reduction in gross output (GO). Concurrently, the model assesses soil damage, considering mechanisms such as erosion, contamination and sedimentation, which may entail additional restoration costs.

The economic module computes the absolute economic damage as the difference between the pre- and post-flood net margin (NM). Net margin is defined as the difference between GO and production costs (PC) over a given production cycle. GO is calculated by multiplying the effective yield by the crop's unit selling price, including direct subsidies (e.g., those provided by the EU's Common Agricultural Policy), while production costs include both variable (e.g., field operations, seeds, fertilizers) and fixed costs. Variations in GO and PC are not only driven by the physical damage itself but also by the post-flood management strategy adopted by the farmer. These may include continuation of cultivation under degraded conditions, crop replanting or complete abandonment of the field, with each pathway implying different cost and revenue structures.

When fully implemented, the AGRIDE-c framework consists of a set of lookup tables that provide, for each crop type, the unitary economic loss (expressed in €/ha)

associated with all possible combinations of flood characteristics, month of occurrence and post-event management strategies.

The main limitation of AGRIDE-c, as with most existing agricultural flood damage models, currently concerns validation, since ex-post agricultural loss data are generally very scarce and fragmented across heterogeneous compensation schemes (e.g., insurance, disaster relief funds, regional aid programs), or lack the level of detail required for robust benchmarking (Merz et al. 2010; Molinari et al. 2019; Faiella 2020; Bremond et al. 2013, 2022; Dang et al. 2024; Lucaora et al. 2025). However, the aim of this study was not to validate a specific damage model, but rather to demonstrate how the proposed integration of seasonal flood probabilities can enhance the interpretability and usefulness of expected loss estimates, regardless of the model employed. In this context, even if different (and eventually validated) seasonally-resolved crop damage models were used, the relative seasonal variability of losses – and, consequently, its influence on cost-benefit outcomes – would remain evident, confirming the robustness of the conceptual findings.

2.5 Implications of accounting for flood seasonality in risk management decisions: insights from a simplified economic scenario

The methodology centers on the computation of the Expected Annual Loss (EAL), a key metric in flood risk analysis and cost-benefit evaluations (Merz et al. 2009; de Moel et al. 2014; Scorzini and Leopardi 2017; Molinari et al. 2021; Yildirim and Demir 2022). The EAL is expressed as follows:

$$EAL = \sum_{j=1}^{N} \Delta P_j \cdot L_j$$

where N is the number of considered flood scenarios with assigned return period, ΔP_j and L_j are, respectively, the exceedance probability increment and average loss of two events with exceedance probabilities (P_j) and (P_{j+1}).

To explore the impact of monthly crop vulnerability on EAL, two alternative formulations of L_j are considered, with the first enabling a probabilistic and phenology-sensitive estimation of flood risk and the second offering a more conservative approach: (i) L_{ave}: monthly-weighted average of flood losses, where each month's contribution is weighted by the corresponding flood probability derived from the regionalized seasonal flood patterns; (ii) L_{max}: maximum monthly loss, corresponding to the most critical crop stage throughout the year.

While the absolute values of expected losses naturally depend on the adopted crop damage model (AGRIDE-c, in this case), the relative differences between L_{ave} and L_{max} are systematic: in this sense, L_{max} can be viewed as analogous to the implementation of a non-seasonal model, whereas L_{ave} provides a more realistic, seasonally explicit representation of expected losses.

A simplified economic evaluation scenario is then conducted to assess the implications associated with the use of each loss formulation. Specifically, the Benefit-Cost Ratio (BCR) is used to assess the maximum level of investment in flood protection that would remain economically feasible to fully avoid agricultural losses across all flood scenarios in the examined area. The BCR is defined as the ratio between the total discounted benefits and costs associated with a mitigation measure over its entire service life (T):

$$BCR = \frac{\sum_{t=0}^{T} \frac{B_t}{(1+r)^t}}{\sum_{t=0}^{T} \frac{C_t}{(1+r)^t}}$$

where B_t and C_t are the benefits and costs in year t and r is the discount rate. In the simplified economic scenario developed for this study, benefits are represented by the total avoided flood damage to crops, corresponding to the EAL accumulated over a supposed 50-years service life of the mitigation measure, starting after its final implementation. Costs are assumed to be incurred upfront, distributed equally over the first two years. The analysis explores two discount rate scenarios, 3% and 5%, and evaluates the BCR as a function of varying investment costs. The BCR is computed under both loss formulations (L_{ave} and L_{max}) to assess how the integration of seasonal crop dynamics influences the perceived cost-effectiveness of flood protection in agricultural areas.

The procedure is applied for illustrative purposes to two adjacent APSFRs (Reno and Panaro rivers) of the Po River district, located in the Emilia-Romagna region (Fig. 2), using the regionalized version of the AGRIDE-c model, adapted to local agronomic conditions within the MOVIDA project (Ballio et al. 2022). The analysis focuses on four major cereal crops (maize, wheat, barley and grassland) identified through the regional agricultural parcel dataset. Under the 100-year return period flood scenario, these crops cover a total exposed area of approximately 286 km².

Based on AGRIDE-c, flood damage for the considered crops is primarily a function of inundation depth and duration. For the application, inundation depth data are derived from available flood hazard maps for three reference return periods (25, 100 and 500 years), while flood duration is uniformly assumed to be under five days, reflecting typical flood characteristics in the region and corresponding

to moderate damage levels during the growing season. As regards inundation depth, the average value for each agricultural plot is computed by intersecting the flood hazard raster with the vector-based cadastral map of agricultural parcels. Moreover, it is assumed that, for each flood scenario, the farmer adopts the minimum-loss response strategy, selected among continuing cultivation, replanting or abandonment.

3 Results and discussion

3.1 Clustering of seasonal flood regimes

The scatter plot in Fig. 3 provides a joint visualization of the classification results of gauged catchments in terms of flood seasonality (y-axis) based on physical descriptors (x-axis) resulting from hierarchical clustering. In the analysis, the number of clusters has been varied systematically and a four-cluster configuration was ultimately retained, offering a good balance between differentiation and interpretability.

Each marker in the plot represents a hydrometric station, color-coded according to the most probable month of seasonal peak discharge occurrence (from January to December). A small random jitter is applied to point coordinates to avoid overplotting and improve readability. The background color shading reflects a smooth spatial interpolation of seasonal peak timing, highlighting gradients and transitions between dominant seasonal regimes across the catchment types and hydrological clusters. Additionally, symbols distinguish stations affected by upstream flow regulation (crosses) from unregulated ones (circles). For visualization purpose, the catchments have been grouped into four physical macro-classes derived from a clustering based on the full set of descriptors listed in Table 1, thus enabling a more accessible comparison of flood seasonality across contrasting physical conditions. More specifically, the four physical classes exhibit distinct characteristics. Class Cpd1 includes the largest catchments, with a wide elevation range and a mean altitude around 800 m a.s.l. In contrast, Class Cpd4 includes smaller basins, generally at lower mean altitudes (ranging from approximately 100 to 1000 m a.s.l.), with moderate slopes and higher internal variability. Classes Cpd2 and Cpd3 represent transitional groups in terms of drainage area, but they are characterized by a more distinctly mountainous setting: Class Cpd2 includes the highest elevation basins, with mean altitudes often exceeding 1400 m a.s.l. and reaching above 2000 m, while Class Cpd3 features catchments typically above 800 m, with maximum mean altitudes around 1000 m a.s.l.

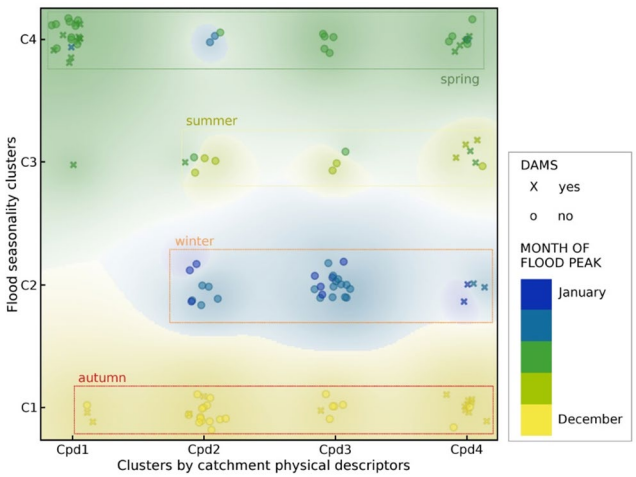

Fig. 3 Classification of gauged catchments into seasonal flood regime clusters, based on empirical monthly flood occurrence probabilities and physical attributes of the catchments.

Overall, the clustering results clearly differentiate the seasonal behavior of peak flows across the gauged stations in the Po River District (Fig. 3): Cluster C1 includes stations with flood peaks mainly occurring in autumn (October to December), C2 in winter (December to March), C3 in summer (May to July), and C4 in spring / spring-autumn (mainly March or late autumn). The most frequent patterns are those with autumn and spring peaks, observed across all classes of catchment physical attributes. These are followed by winter peaks, while summer peaks are limited to a smaller number of locations whose hydrological response is primarily driven by more delayed snowmelt processes.

For each of the identified clusters, a representative seasonal flood pattern is derived in terms of the monthly probability of annual peak flow occurrence (thick black lines represented in Fig. 4). These cluster-specific patterns are computed as the average of the observed monthly distributions at the gauged stations (thin gray-scale lines in Fig. 4) belonging to each cluster, thus capturing the typical temporal profile of flood hazard associated with different physical conditions of the catchments.

3.2 Regionalization to ungauged catchments

Figure 5 illustrates the final spatial mapping of flood seasonality clusters across the entire Po River District, as obtained from the supervised machine learning models described in Sect. 2.3.2. Specifically, the map in Fig. 5a shows the classification results obtained using SVM, which yielded the best performance among the tested models. In detail, the SVM achieved an average classification accuracy of 0.64 (with a precision of 0.58) on the test set, while the other two models (KNN and RF) had slightly lower performance, with accuracies around 0.55 (precision of 0.51). Although these values may be considered modest, they are consistent with the inherent complexity of the classification task under analysis

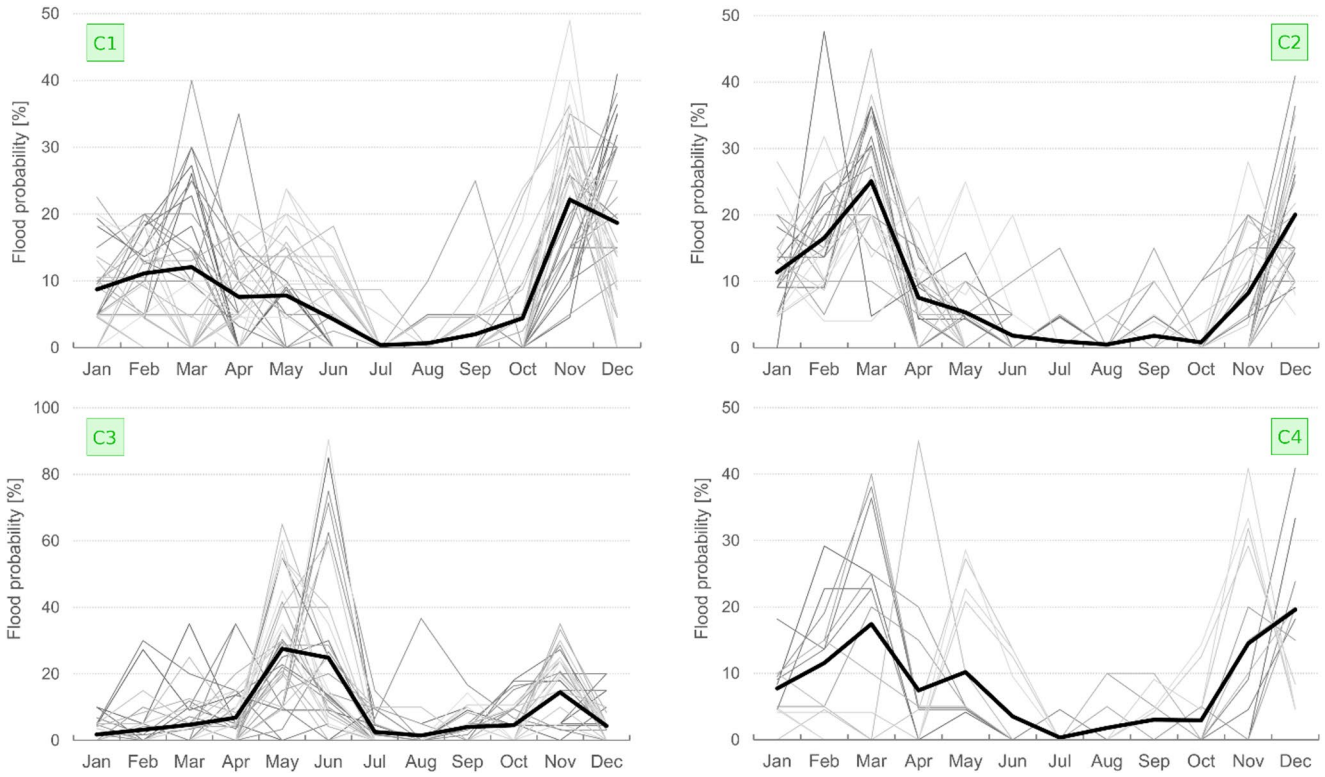

Fig. 4 Monthly flood probability profiles for each seasonal cluster (C1: autumn peaks; C2: winter peaks; C3: summer peaks; C4: spring / spring-autumn peaks). Thin grey lines show individual gauged catchments; thick black lines indicate the average pattern per cluster.

(characterized by gradual transitions among classes), further complicated by the limited size of the training dataset available for the study area. Additionally, it is worth noting that the model design intentionally prioritized simplicity to support large-scale applicability, relying solely on a limited set of physical descriptors that, although widely available and straightforward to compute, may not be able to fully capture the hydrologic response of a catchment (Merz and Blöschl 2009).

To provide a more quantitative assessment of model performance and internal uncertainty, Fig. 6 reports the confusion matrices for the three classifiers, allowing a detailed inspection of class-wise accuracy and misclassification patterns. The results in Fig. 6 confirm, on one hand, the superior performance of SVM, which achieves higher true positive rates across all seasonal clusters, and, on the other hand, the tendency of misclassifications to concentrate between adjacent transitional regimes (i.e., autumn-winter and summer identified as spring or autumn), reflecting the inherently less distinct boundaries of these intermediate conditions.

To enhance the interpretability and confidence in the spatial classification, the results of the ensemble-consensus strategy adopted in this study are reported in Fig. 5b, which highlights the areas with consistent or divergent model predictions. Catchments shown in light blue-green are those for which at least one of the two alternative models (KNN or RF) returned the same cluster as the SVM. Conversely, areas with inconsistent predictions are displayed with a pink dashed fill. In these cases, the cluster label indicated on the map corresponds to the one jointly predicted by the two alternative models, which always agreed with each other in all reported cases. As previously noted in the test set, most of the differences shown in Fig. 5b are again between autumn and winter clusters, further emphasizing the challenge of clearly delineating seasonality regimes in transitional contexts.

The spatial pattern represented in Fig. 5 reveals a clear zonation reflecting both climatic and physiographic gradients in the area. Class 1 (red regions), dominated by autumn flood peaks, is primarily associated with the Apennine areas in the southern sector of the Po district, as well as with several sub-catchments in the western and central Alpine foothills. These areas are typically characterized by strong influence of Mediterranean cyclonic activity in the autumn months, which often brings intense precipitation events over steep, rapidly responding catchments (Brath et al. 2006).

Class 2 (orange regions), which includes sub-catchments with winter flood peaks, forms a continuous belt across the central Po Plain and along the inner Alpine slopes. This pattern reflects the role of winter frontal systems and low-intensity but long-duration rainfall events, often combined with snowmelt contributions in lower-altitude alpine and

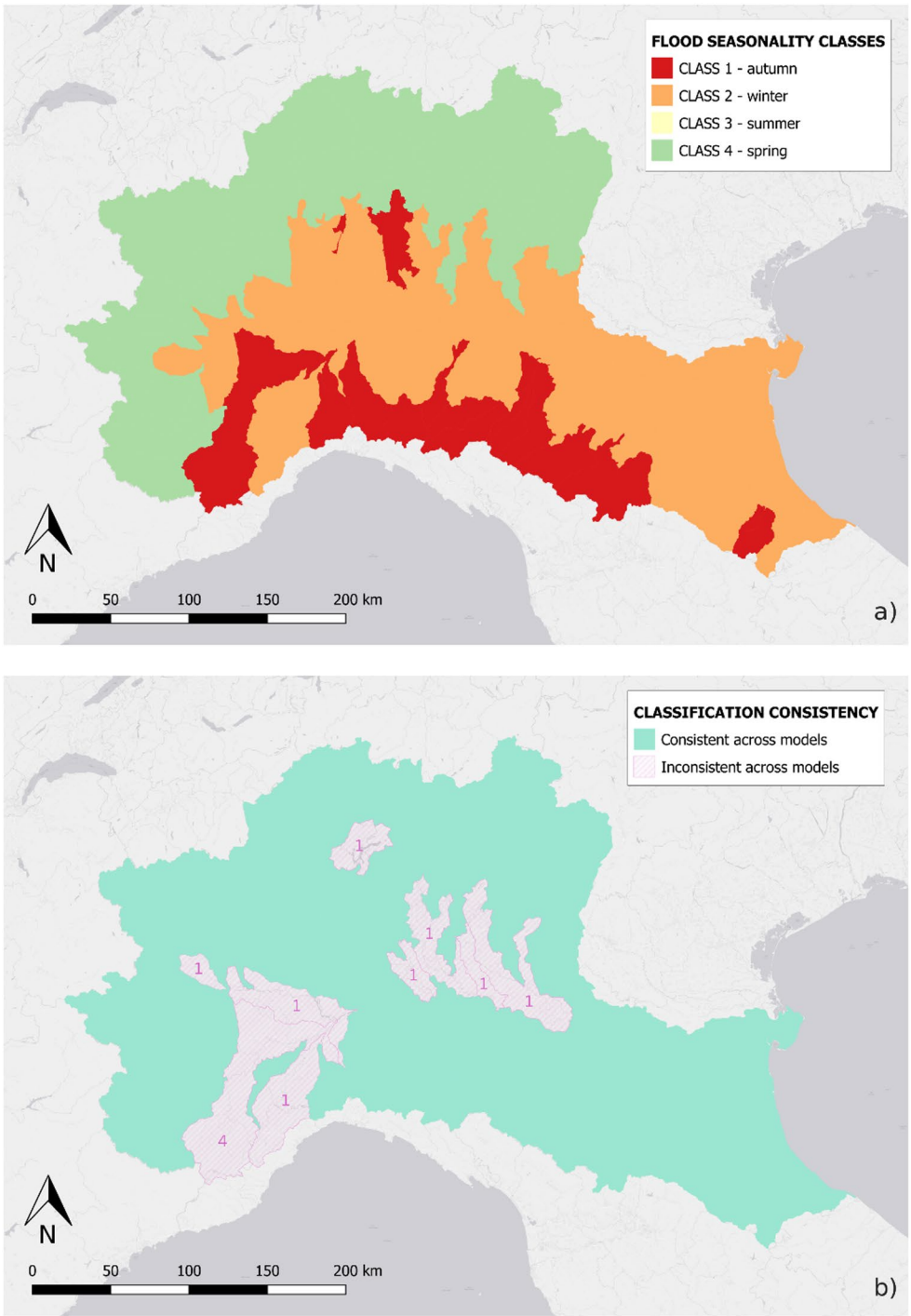

Fig. 5 **a** Predicted seasonal flood regime clusters across the sub-catchment of the Po River District using the SVM classifier. **b** Model agreement map: areas with consistent predictions across classifiers are shown in blue-green; inconsistent areas in pink, with numbers indicating the class jointly predicted by the two agreeing models.

pre-alpine basins during warmer winter periods (Coppola et al. 2014).

Class 4 (green regions), representing spring-dominated flood regimes, mainly occurs in the northern part of the district, particularly in the high-altitude areas of the western and central Alps. These zones are typically influenced by snow accumulation during winter, followed by a spring melt, leading to increased runoff and peak flows in spring (De Michele and Rosso 2002; Kormann et al. 2015). Class 3, corresponding to summer flood seasonality (yellow areas), is absent in the final classification map. This absence may be attributed to the limited number of gauged catchments exhibiting a distinct summer flood regime in the training dataset, which likely reduced the classifier's ability to identify this class. Moreover, in high-altitude alpine areas, the seasonal transition between spring and early summer flood peaks is often gradual and sensitive to interannual variability in snowmelt dynamics and rainfall events. As a result,

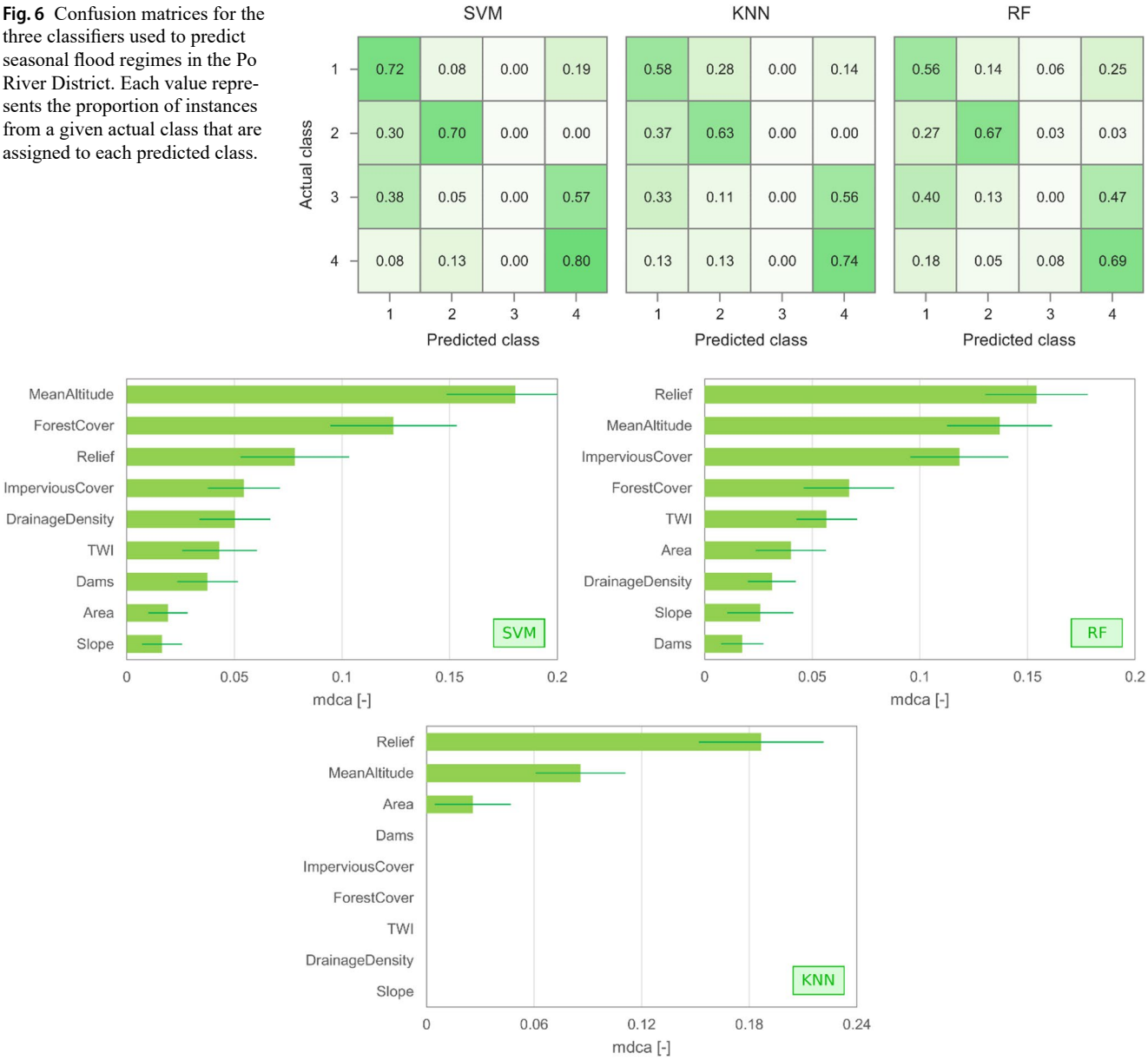

Fig. 6 Confusion matrices for the three classifiers used to predict seasonal flood regimes in the Po River District. Each value represents the proportion of instances from a given actual class that are assigned to each predicted class.

Fig. 7 Feature importance for SVM, RF and KNN classifiers. The features are ranked in descending order of importance, as measured by the mean decrease in classification accuracy (mdca), with the error bars reporting the corresponding standard deviations.

some basins that were classified as spring-dominated (Class 4) may in fact exhibit characteristics more consistent with a summer regime (De Michele and Rosso 2002; Soncini and Bocchiola 2011; Kormann et al. 2015; Blöschl et al. 2017).

The analysis based on the mean decrease in classification accuracy (mdca) offers further insights into the key physical drivers shaping the seasonal flood regime classes across the study area (Fig. 7). Despite some variability among the models, certain patterns are consistently observed. For the SVM classifier, the most influential variables are MeanAltitude, ForestCover and Relief, which together suggest a dominant role of catchment-scale orographic and land cover features on flood seasonality. The influence of ImperviousCover and DrainageDensity is moderate, while topographic and morphometric descriptors (such as TWI, Slope and Area), as well as the indicator for the presence of dams, show lower importance values. The RF model exhibits a slightly different pattern, with Relief and MeanAltitude again emerging as the leading predictors, but ImperviousCover also showing a comparable relevance. ForestCover and TWI maintain an intermediate role, while the presence of Dams and other morphometric features have relatively minor effects. The KNN classifier produces a more selective feature ranking, clearly prioritizing Relief, MeanAltitude and Area, while

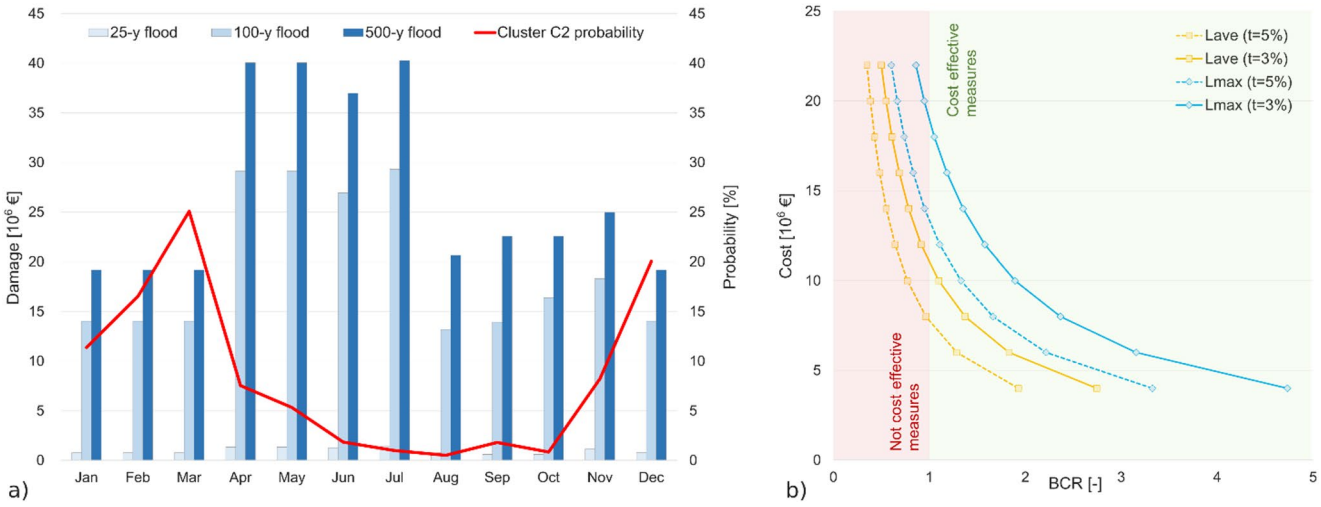

Fig. 8 Effect of flood seasonality on the results of crop damage modeling and cost-benefit analysis for the simplified economic scenario in the Panaro-Reno system: **a** Time-varying expected losses for the considered synthetic flood scenarios with 25, 100 and 500-years return period; **b** BCR trends by investment cost, comparing L_{max} and L_{ave} formulations under 3% and 5% discount rates

the remaining variables contribute little to model accuracy. This outcome is in line with the nature of KNN models, which can be more sensitive to a subset of dominant features (Tang et al. 2014; García et al. 2015).

Overall, the results highlight the importance of elevation-related descriptors as key determinants of flood seasonality at the district scale. These findings support the hydrological relevance of catchment altitude and relief in modulating snowmelt contribution, precipitation patterns and runoff dynamics. The moderate but recurrent contribution of ImperviousCover and ForestCover across models also suggests a non-negligible influence of land use, especially in terms of runoff generation and attenuation processes.

3.3 Implications of accounting for flood seasonality in risk management decisions: insights from a simplified economic scenario

Figure 8 summarizes the impact of incorporating flood seasonality into agricultural risk estimation, highlighting the differences in computed losses and their implications for cost-benefit analysis for the illustrative example of the Panaro-Reno system, located in Cluster 2. As shown in the left panel (Fig. 8a), the most severe crop losses (L_{max}) occur for flood events between April and July, with the absolute maximum observed in July. In this month, expected losses range from approximately €1.7 million for the 25-year return period flood to €29.6 million and €40.6 million for the 100-year and 500-year scenarios, respectively.

However, when losses are weighted by the seasonal flood probability (L_{ave}) derived for Cluster C2 (Fig. 4), the resulting average annual losses are significantly lower - about €1.2 million, €17.0 million and €23.5 million, respectively, for the three considered return periods. These differences directly affect the EAL, yielding approximately €750,000 under the L_{max} formulation and €435,000 when using L_{ave}.

A simplified cost-benefit analysis has been then conducted to assess the potential implications of such differences on decisions about investments in risk mitigation. The analysis considers a hypothetical (ideal) scenario in which a structural mitigation measure completely eliminates agricultural flood damage in the study area. The BCR is used to identify the maximum economically feasible investment, assuming a service life of 50 years, with costs distributed evenly over the first 2 years and a fixed discount rate ranging between 3 and 5%. The results, shown in Fig. 8b, indicate that economically efficient interventions (BCR > 1) would be feasible for costs up to approximately €7–12 million when using the L_{ave} formulation (yellow lines), and up to €13–20 million when using L_{max} (blue lines), depending on the selected discount rate.

To further explore the potential impact of uncertainty in seasonal flood classification on cost-benefit analysis outcomes, the BCR under the L_{ave} formulation was recalculated considering the possible misclassification of the winter cluster (C2) toward the autumn class (C1), as indicated by confusion matrices in Fig. 6. In these cases, the maximum economically feasible investment for a BCR = 1 shifted from €7.7 million (discount rate t = 5%) and €11.0 million (t = 3%), when using the winter probability distribution, to €8.3 million (t = 5%) and €11.8 million (t = 3%) under the autumn distribution. Even though the resulting differences are relatively small in absolute terms, they demonstrate that uncertainties arising from the regionalization step can propagate through the entire risk assessment chain, ultimately affecting economic indicators such as the BCR. The

magnitude of this influence is expected to be context-dependent, varying according to both the regional distribution of flood probabilities and the characteristics of local cropping systems, whose phenological stages determine the temporal pattern of vulnerability.

Building on this consideration, while the presented application remains illustrative and based on simplified assumptions rather than on a fully validated case study, the findings still demonstrate that the choice of damage formulation - whether or not it accounts for the seasonal dynamics of crop vulnerability - can substantially affect perceived cost-effectiveness and guide investment prioritization in agricultural flood protection. They underscore, on one hand, the importance of employing crop damage models that explicitly account for the timing of flood events throughout the year, and, on the other hand, the value of incorporating regionalized monthly flood probabilities and uncertainty quantification into risk assessments. This combined approach contributes to more balanced and informed investment decisions, reducing the likelihood of overly cautious strategies that may lead to inefficient allocation of resources, while still ensuring adequate protection of agricultural assets.

4 Conclusions

This study developed and tested a methodological framework that explicitly incorporates flood seasonality into agricultural risk assessments, offering a scalable solution to the challenges posed by spatial heterogeneity and data scarcity in large river basins. By combining unsupervised clustering with supervised machine learning, the framework enables the regionalization of seasonally-resolved flood regimes, generating monthly flood probability profiles that can be spatially transferred to ungauged catchments.

First, catchments are grouped into seasonal flood regime classes using unsupervised clustering of empirical monthly flood occurrence probabilities, derived from long-term streamflow observations. These clusters capture distinct intra-annual flood mechanisms, shaped by physical and anthropogenic factors. Second, supervised classification models are trained to predict the seasonal regime class in ungauged basins relying solely on catchments' physical attributes. In the illustrative example for the Po River District, among the tested algorithms, Support Vector Machines provided the most robust classification performance, even though the results indicated inherent challenges in modeling transitional seasonal regimes. The variable importance analysis consistently highlighted elevation-dependent and land-use attributes (such as forest cover) as key predictors of flood seasonality, providing valuable insights into its physical controls in the investigated area.

The resulting output of the regionalization procedure (spatially distributed monthly flood probability profiles) serves as a key input to agricultural damage modeling. The integration with the AGRIDE-c model enables probabilistic estimation of flood losses that explicitly accounts for both seasonal hazard patterns and crop phenology. The simplified economic scenario illustrated in this study demonstrated the added value of integrating flood seasonality into risk metrics. The comparison between seasonal and non-seasonal loss formulations showed that ignoring the temporal distribution of floods and crop sensitivity can lead to significantly inflated risk estimates and potentially suboptimal mitigation planning. When integrated into cost-benefit analyses, the seasonally-aware estimates can indeed provide a more balanced perspective on investment feasibility, helping to avoid over-dimensioned interventions while ensuring sufficient protection of agricultural assets.

Overall, the findings highlighted the importance of advancing beyond static representations of hazard and vulnerability in flood risk assessments. The proposed approach represents a step forward in this direction, offering operational tools to improve the reliability and relevance of flood risk assessments in agricultural landscapes, particularly in support of climate adaptation and disaster risk reduction policies.

Nonetheless, certain limitations remain, particularly regarding the inherent uncertainty of the regionalization process and the need for fully validated damage models. Future developments should additionally focus on testing the framework in different hydro-climatic and agronomic settings, examining how uncertainties propagate across the workflow and assessing the sensitivity of policy-relevant indicators to alternative model configurations. Such efforts would further consolidate the robustness of the framework and support its broader operational application.

Author contributions Anna Rita Scorzini: Conceptualization; Methodology; Data curation; Formal analysis; Investigation; Visualization; Writing - original draft.Charlie Dayane Paz Idarraga: Data curation; Formal analysis.Daniela Molinari: Conceptualization; Investigation; Writing - review and editing.

Funding Open access funding provided by Università degli Studi dell'Aquila within the CRUI-CARE Agreement. This work was supported by Autorità di Bacino Distrettuale del Fiume Po under the MOVIDA agreement.

Data availability No datasets were generated or analysed during the current study.

Declarations

Competing interests The authors declare no competing interests.

References

Ballio F, Armaroli C, Arosio M, Arrighi C, Mondino EB, Carisi F, Zoppi L (2022) The movida project to support the update of flood risk maps in the Po River District: methodology for flood damage assessment. In: Proceedings of the 39th IAHR World Congress - From Snow To Sea, Granada, Spain (pp. 6653–6657). ISSN: 2521-716X https://doi.org/10.3850/IAHR-39WC2521711920221136

Blöschl G, Sivapalan M, Wagener T, Viglione A, Savenije H (2013) Runoff prediction in ungauged basins: synthesis across processes, places and scales. Cambridge University Press, Cambridge, UK, 465p. ISBN: 978-1-107-02818-0

Blöschl G, Hall J, Parajka J, Perdigão RA, Merz B, Arheimer B, ivković N (2017) Changing climate shifts timing of European floods. Science 357(6351):588–590. https://doi.org/10.1126/science.aan2506

Bormann H (2010) Towards a hydrologically motivated soil texture classification. Geoderma 157(3–4):142–153. https://doi.org/10.1016/j.geoderma.2010.04.005

Bormann H, Diekkrüger B, Renschler C (1999) Regionalisation concept for hydrological modelling on different scales using a physically based model: results and evaluation. Phys Chem Earth Part B Hydrol Oceans Atmos 24(7):799–804. https://doi.org/10.1016/S1464-1909(99)00083-0

Brath A, Montanari A, Moretti G (2006) Assessing the effect on flood frequency of land use change via hydrological simulation (with uncertainty). J Hydrol 324(1–4):141–153. https://doi.org/10.1016/j.jhydrol.2005.10.001

Breiman L (2001) Random forests. Mach Learn 45:5–32. https://doi.org/10.1023/A:1010933404324

Bremond P, Grelot F, Agenais AL (2013) Economic evaluation of flood damage to agriculture–review and analysis of existing methods. Nat Hazards Earth Syst Sci 13(10):2493–2512. https://doi.org/10.5194/nhess-13-2493-2013

Bremond P, Agenais AL, Grelot F, Richert C (2022) Process-based flood damage modelling relying on expert knowledge: a methodological contribution applied to agricultural sector. Nat Hazards Earth Syst Sci 22(10):3385–3412. https://doi.org/10.5194/nhess-22-3385-2022

Buttle J (2006) Mapping first-order controls on streamflow from drainage basins: the T^3 template. Hydrol Processes 20(15):3415–3422. https://doi.org/10.1002/hyp.6519

Coopersmith E, Yaeger MA, Ye S, Cheng L, Sivapalan M (2012) Exploring the physical controls of regional patterns of flow duration curves-Part 3: a catchment classification system based on regime curve indicators. Hydrol Earth Syst Sci 16(11):4467–4482. https://doi.org/10.5194/hess-16-4467-2012

Coppola E, Verdecchia M, Giorgi F, Colaiuda V, Tomassetti B, Lombardi A (2014) Changing hydrological conditions in the Po basin under global warming. Sci Total Environ 493:1183–1196. https://doi.org/10.1016/j.scitotenv.2014.03.003

Cortes C, Vapnik V (1995) Support-vector networks. Mach Learn 20:273–297. https://doi.org/10.1007/BF00994018

Cover T, Hart P (1967) Nearest neighbor pattern classification. IEEE Trans Inf Theory 13(1):21–27. https://doi.org/10.1109/TIT.1967.1053964

Dang Y, Yang L, Song J (2024) The construction of a crop flood damage assessment index to rapidly assess the extent of postdisaster impact. Remote Sens 16(9):1527. https://doi.org/10.3390/rs16091527

De Michele C, Rosso R (2002) A multi-level approach to flood frequency regionalisation. Hydrol Earth Syst Sci 6(2):185–194. https://doi.org/10.5194/hess-6-185-2002

de Moel H, Bouwer LM, Aerts JC (2014) Uncertainty and sensitivity of flood risk calculations for a dike ring in the South of the Netherlands. Sci Total Environ 473:224–234. https://doi.org/10.1016/j.scitotenv.2013.12.015

Drissia TK, Jothiprakash V, Sivakumar B (2022) Regional flood frequency analysis using complex networks. Stoch Env Res Risk A 36(1):115–135. https://doi.org/10.1007/s00477-021-02074-1

Faiella A (2020) Agriculture damage data collection: a model for reconstructing comprehensive damage dynamics. Prog Disaster Sci 7:100112. https://doi.org/10.1016/j.pdisas.2020.100112

FAO (2023) The impact of disasters on agriculture and food security 2023—avoiding and reducing losses through investment in resilience. Rome. https://doi.org/10.4060/cc7900en. ISBN 978-92-5-138194-6

Fathi MM, Awadallah AG (2025) Regionalizing hydrologic information for runoff predictions beyond continental boundaries using machine learning. Adv Water Resour 105162. https://doi.org/10.1016/j.advwatres.2025.105162

Förster S, Kuhlmann B, Lindenschmidt KE, Bronstert A (2008) Assessing flood risk for a rural detention area. Nat Hazards Earth Syst Sci 8(2):311–322. https://doi.org/10.5194/nhess-8-311-2008

Gao M, Chen X, Liu J, Zhang Z (2018) Regionalization of annual runoff characteristics and its indication of co-dependence among hydro-climate–landscape factors in Jinghe river Basin, China. Stoch Env Res Risk A 32(6):1613–1630. https://doi.org/10.1007/s00477-017-1494-9

García S, Luengo J, Herrera F (2015) Data preprocessing in data mining. Springer, Cham, Switzerland. 320p. ISBN 978-3-319-10247-4. https://doi.org/10.1007/978-3-319-10247-4

Kim W, Iizumi T, Hosokawa N, Tanoue M, Hirabayashi Y (2023) Flood impacts on global crop production: advances and limitations. Environ Res Lett 18(5):054007. https://doi.org/10.1088/1748-9326/accd85

Kormann C, Francke T, Renner M, Bronstert A (2015) Attribution of high resolution streamflow trends in Western Austria–an approach based on climate and discharge station data. Hydrol Earth Syst Sci 19(3):1225–1245. https://doi.org/10.5194/hess-19-1225-2015

Kuentz A, Arheimer B, Hundecha Y, Wagener T (2017) Understanding hydrologic variability across Europe through catchment classification. Hydrol Earth Syst Sci 21(6):2863–2879. https://doi.org/10.5194/hess-21-2863-2017

Lazzarin T, Viero DP, Molinari D, Ballio F, Defina A (2022) A new framework for flood damage assessment considering the within-event time evolution of hazard, exposure, and vulnerability. J Hydrol 615:128687. https://doi.org/10.1016/j.jhydrol.2022.128687

Lucaora T, Annis A, Nardi F, Rulli MC, Chiarelli DD (2025) Distributed hydrodynamic modelling for assessing flood impacts on crops: assessing flood-resilient crop management in a coastal basin of central Italy. Agric Water Manag 309:109352. https://doi.org/10.1016/j.agwat.2025.109352

Merz R, Blöschl G (2004) Regionalisation of catchment model parameters. J Hydrol 287(1–4):95–123. https://doi.org/10.1016/j.jhydrol.2003.09.028

Merz R, Blöschl G (2009) A regional analysis of event runoff coefficients with respect to climate and catchment characteristics in Austria. Water Resour Res 45(1):W01405. https://doi.org/10.1029/2008WR007163

Merz B, Elmer F, Thieken AH (2009) Significance of high probability/low damage versus low probability/high damage flood events. Nat Hazards Earth Syst Sci 9(3):1033–1046. https://doi.org/10.5194/nhess-9-1033-2009

Merz B, Kreibich H, Schwarze R, Thieken A (2010) Review Article assessment of economic flood damage. Nat Hazards Earth Syst Sci 10(8):1697–1724. https://doi.org/10.5194/nhess-10-1697-2010

Molinari D, Scorzini AR, Gallazzi A, Ballio F (2019) AGRIDE-c, a conceptual model for the Estimation of flood damage to crops: development and implementation. Nat Hazards Earth Syst Sci 19(11):2565–2582. https://doi.org/10.5194/nhess-19-2565-2019

Molinari D, Dazzi S, Gattai E, Minucci G, Pesaro G, Radice A, Vacondio R (2021) Cost–benefit analysis of flood mitigation measures: a case study employing high-performance hydraulic and damage modelling. Nat Hazard 108(3):3061–3084. https://doi.org/10.1007/s11069-021-04814-6

Montanari A (2012) Hydrology of the Po river: looking for changing patterns in river discharge. Hydrol Earth Syst Sci 16(10):3739–3747. https://doi.org/10.5194/hess-16-3739-2012

Rao AR, Srinivas VV (2006) Regionalization of watersheds by hybrid-cluster analysis. J Hydrol 318(1–4):37–56. https://doi.org/10.1016/j.jhydrol.2005.06.003

Rao AR, Srinivas VV (2008) Regionalization of watersheds: an approach based on cluster analysis. Springer Dordrecht, The Netherlands. 250p. ISBN: 978-1-4020-6852-2. https://doi.org/10.1007/978-1-4020-6852-2

Razavi T, Coulibaly P (2013) Classification of Ontario watersheds based on physical attributes and streamflow series. J Hydrol 493:81–94. https://doi.org/10.1016/j.jhydrol.2013.04.013

Salinas JL, Laaha G, Rogger M, Parajka J, Viglione A, Sivapalan M, Blöschl G (2013) Comparative assessment of predictions in ungauged basins-Part 2: flood and low flow studies. Hydrol Earth Syst Sci 17(7):2637–2652. https://doi.org/10.5194/hess-17-2637-2013

Sawicz K, Wagener T, Sivapalan M, Troch PA, Carrillo G (2011) Catchment classification: empirical analysis of hydrologic similarity based on catchment function in the Eastern USA. Hydrol Earth Syst Sci 15(9):2895–2911. https://doi.org/10.5194/hess-15-2895-2011

Scorzini AR, Leopardi M (2017) River basin planning: from qualitative to quantitative flood risk assessment: the case of Abruzzo region (central Italy). Nat Hazard 88:71–93. https://doi.org/10.1007/s11069-017-2857-8

Scorzini AR, Di Bacco M, Manella G (2021) Regional flood risk analysis for agricultural crops: insights from the implementation of AGRIDE-c in central Italy. Int J Disaster Risk Reduct 53:101999. https://doi.org/10.1016/j.ijdrr.2020.101999

Sivakumar B, Singh VP (2012) Hydrologic system complexity and nonlinear dynamic concepts for a catchment classification framework. Hydrol Earth Syst Sci 16(11):4119–4131. https://doi.org/10.5194/hess-16-4119-2012

Soncini A, Bocchiola D (2011) Assessment of future snowfall regimes within the Italian alps using general circulation models. Cold Reg Sci Technol 68(3):113–123. https://doi.org/10.1016/j.coldregions.2011.06.011

Sørensen R, Zinko U, Seibert J (2006) On the calculation of the topographic wetness index: evaluation of different methods based on field observations. Hydrol Earth Syst Sci 10(1):101–112. https://doi.org/10.5194/hess-10-101-2006

Tang J, Alelyani S, Liu H (2014) Feature selection for classification: a review. In: Data classification: algorithms and applications, CRC Press, pp 37–64. ISBN: 9781466586758

Tarquini S, Isola I, Favalli M, Battistini A, Dotta G (2023) TINITALY, a Digital elevation model of Italy with a 10 meters cell size (Version 1.1). Istituto nazionale Di geofisica e vulcanologia (INGV). https://doi.org/10.13127/tinitaly/1.1

Vozinaki AEK, Karatzas GP, Sibetheros IA, Varouchakis EA (2015) An agricultural flash flood loss Estimation methodology: the case study of the Koiliaris basin (Greece), February 2003 flood. Nat Hazard 79:899–920. https://doi.org/10.1007/s11069-015-1882-8

Wagener T, Sivapalan M, Troch P, Woods R (2007) Catchment classification and hydrologic similarity. Geogr Compass 1(4):901–931. https://doi.org/10.1111/j.1749-8198.2007.00039.x

Winter TC (2001) The concept of hydrologic landscapes. JAWRA J Am Water Resour Assoc 37(2):335–349. https://doi.org/10.1111/j.1752-1688.2001.tb00973.x

Wolock DM, Winter TC, McMahon G (2004) Delineation and evaluation of hydrologic-landscape regions in the united States using geographic information system tools and multivariate statistical analyses. Environ Manag 34:S71–S88. https://doi.org/10.1007/s00267-003-5077-9

Yildirim E, Demir I (2022) Agricultural flood vulnerability assessment and risk quantification in Iowa. Sci Total Environ 826:154165. https://doi.org/10.1016/j.scitotenv.2022.154165